

**Supporting information for  
“High-throughput mutate-map-rescue evaluates SHAPE-directed RNA structure  
and uncovers excited states”**

Siqi Tian,<sup>1</sup> Pablo Cordero,<sup>2</sup> Wipapat Kladwang,<sup>3</sup> and Rhiju Das<sup>1, 2, 3, \*</sup>

<sup>1</sup>Department of Biochemistry, <sup>2</sup>Biomedical Informatics Program, and <sup>3</sup>Department of Physics, Stanford University, Stanford, California 94305, United States

\*Corresponding Author

This document contains the following sections:

Supporting Figures S1-S6

Supporting Tables S1-S2

Supporting References

## SUPPORTING FIGURES

**Figure S1. Confirming sequence assignments and comparisons of SHAPE/DMS/CMCT modeling.** (A) Electropherogram of SHAPE and ddNTP ladder co-loading. Sequence assignment is marked on top. Since reverse transcriptase is blocked prior to acylation and ddNTP termination occurs after the incorporation, there is a single register shift for the same nucleotide across profiles. (B) Normalized SHAPE reactivity derived from capillary electrophoresis (CE) and next-generation sequencing (MAP-Seq). Standard deviations (SD) are shown, N = 7 for CE, N = 2 MAP-Seq. (C) Secondary structure prediction of 126-235 RNA without data guidance. (D-E) Secondary structure prediction and bootstrap support matrix using 1-dimensional DMS/CMCT data. For A and C residues, DMS reactivity is taken; and for G and U residues, CMCT reactivity is taken. The model contains a different version of helices compared to 1D-data-guided model, labeled as alt-P4' and alt-P5' respectively. Difference from crystallographic model is drawn in yellow/gray lines. Percentage labels give bootstrap support values.

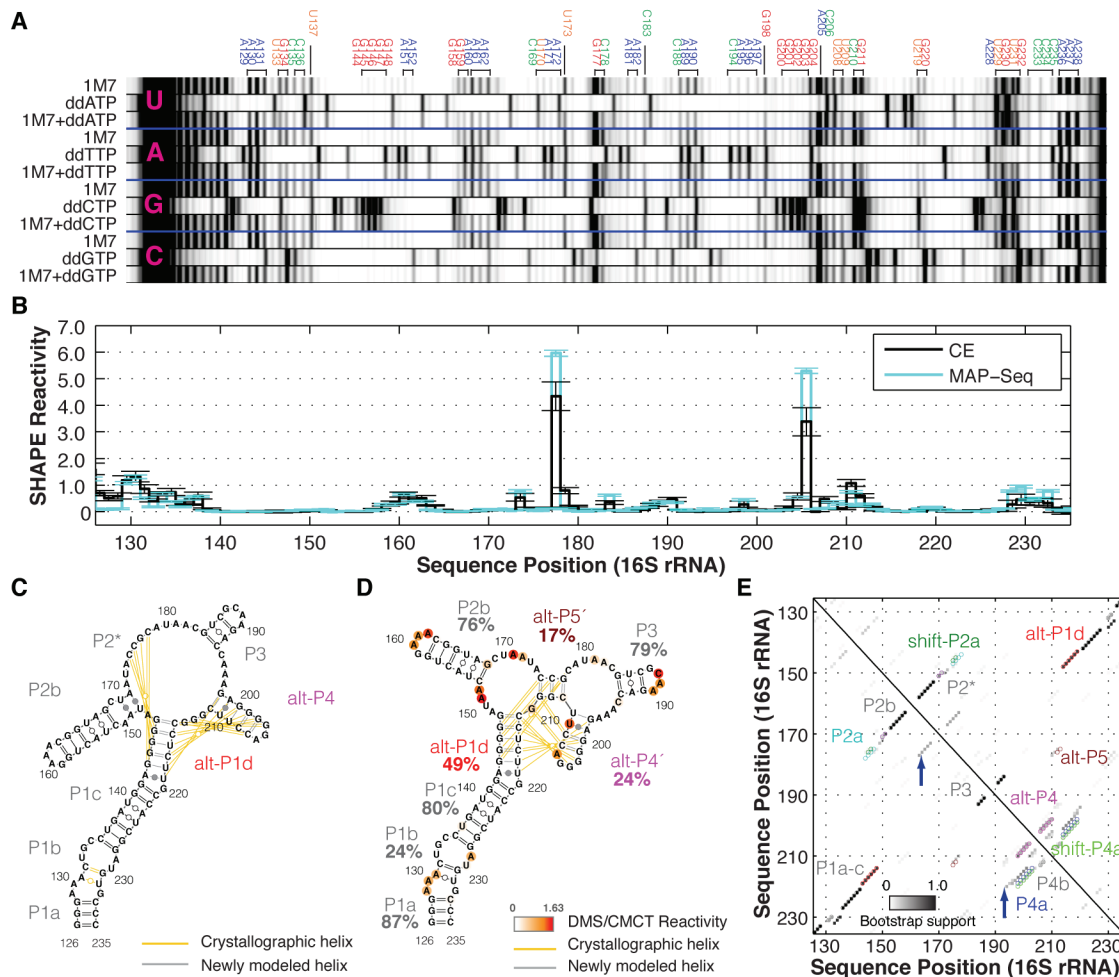


**Figure S2 (next page). Consistent but uncertain SHAPE-directed models from different data processing software, secondary structure software and experimental conditions.** (A) Similar normalized SHAPE reactivities from different data processing packages. Flanking sequences are grayed and GAGUA pentaloop (Kladwang et al. 2014) highlighted in yellow. (B-K) Secondary structure predictions and bootstrap support matrices using variants of the SHAPE analysis match default analysis (Figure 2A-B). (B-C) Data processed by QuSHAPE give results consistent with default HiTRACE analysis. (D-E) Data normalized so that mean reactivity of flanking GAGUA pentaloops are set to 1.0 instead of 2.0 (default procedure to match prior work; see Methods), gives results consistent with default analysis. (F-G) Data normalized as described in (Deigan et al. 2009) do not give alt-P5a, which is present but with low bootstrap support value (13%) in default analysis. (H-I) Use of RNAsstructure version 5.5 (Hajdin et al. 2013) instead of version 5.4 (Deigan et al. 2009) gives a similar secondary structure model but with high confidence in helices alt-P1d and alt-P4, which are falsified by independent data (see main text). (J-K) Inclusion of 200 mM KOAc (with 10 mM MgCl<sub>2</sub> and 50 mM Na-HEPES, pH 8.0) during SHAPE probing, to match (Deigan et al. 2009), gives results consistent with default solution conditions without added KOAc; see (M). Difference from crystallographic model is drawn in yellow/gray lines. Percentage labels give bootstrap support values. (L) Data using dGTP vs. dITP in reverse transcription can give different systematic effects at G vs. C positions (Kladwang et al. 2011), but give data in close agreement for the 126-235 RNA. Asterisks mark bands with variable background. (M) Normalized SHAPE reactivity of wild-type 126-235 RNA under different folding conditions.

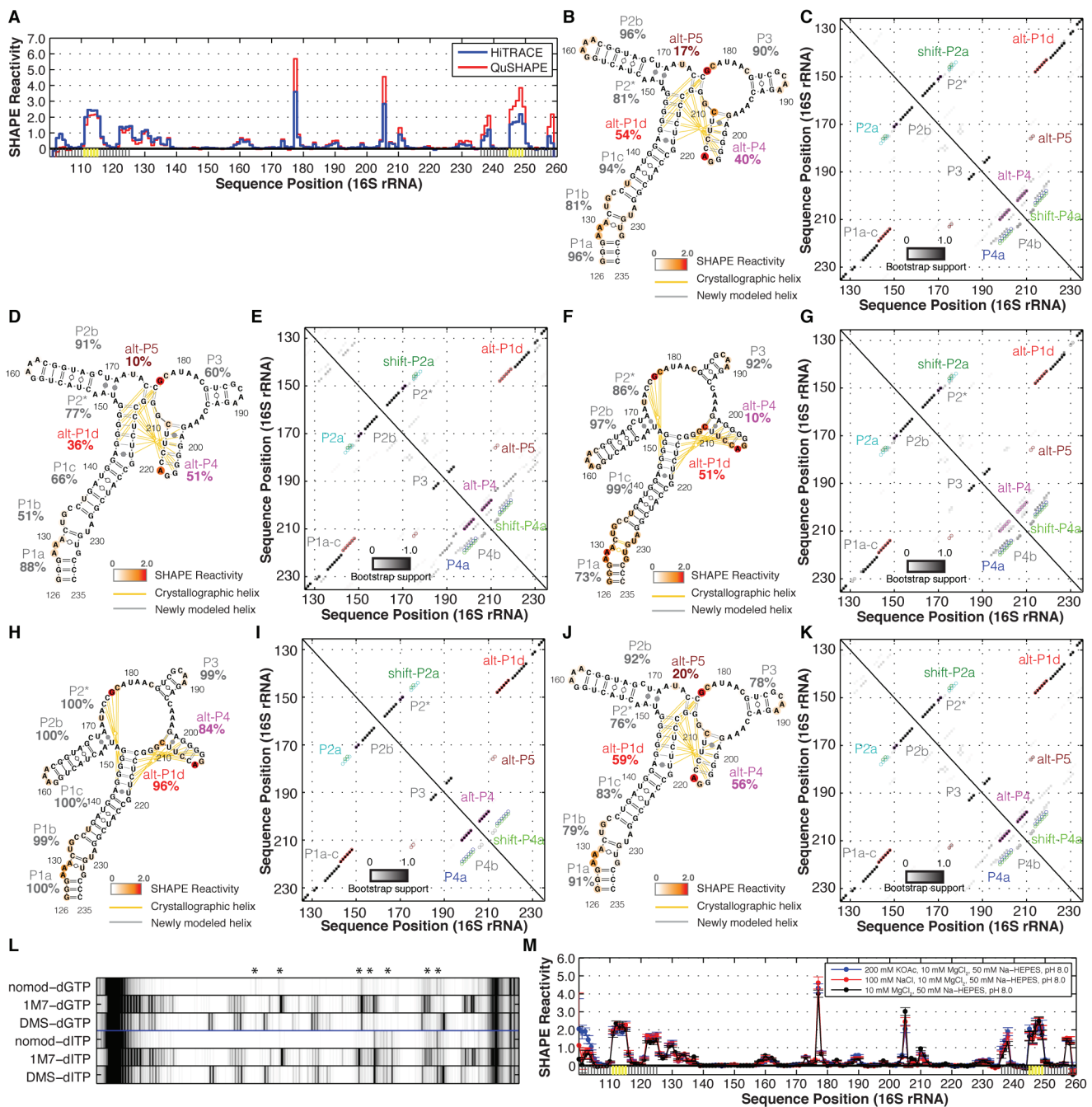


**Figure S3. Mutate-and-map ( $M^2$ ) data of 126-235 RNA using 1M7 and DMS modifiers give consistent results as NMIA  $M^2$  analysis.** (A) Entire mutate-and-map dataset (1M7) across 110 single mutations. (B) Z-score contact-map extracted from (A), used for secondary structure inference. (C-D) Secondary structure prediction and bootstrap support matrix using 2-dimensional  $M^2$  data (1M7). (E-F) Entire mutate-and-map dataset (DMS) and Z-score contact-map. (G-H) Secondary structure prediction and bootstrap support matrix using 2-dimensional  $M^2$  data (DMS). The model contains a different version of helix compared to 2D-data-guided model, labeled as shift-P2a'. Difference from crystallographic model is drawn in yellow/gray lines. Percentage labels give bootstrap support values.

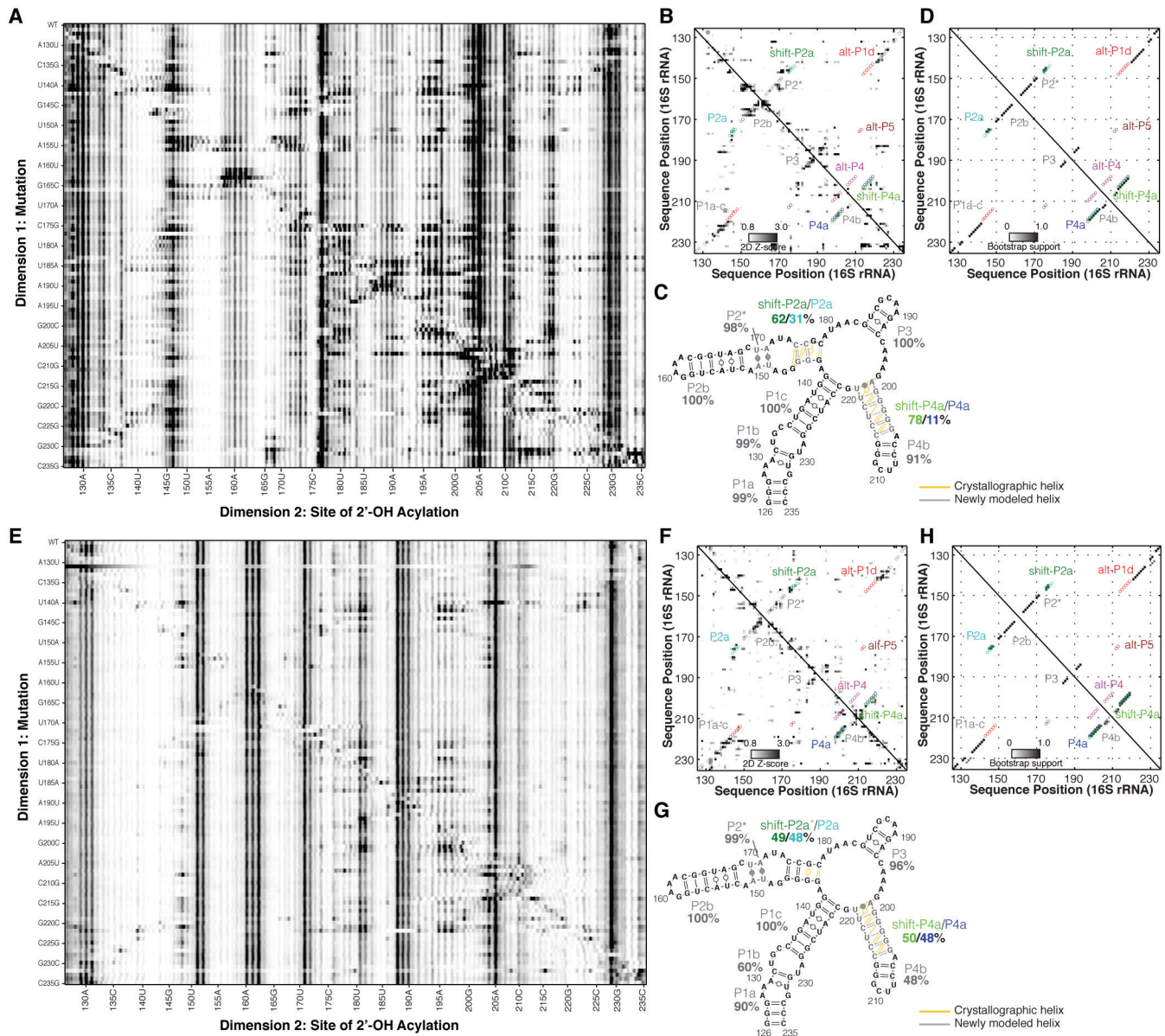


**Figure S4. Overlays of compensatory mutants test modeled secondary structures and allow tests of proposed P4a helix register shift.** (A, E) Compensatory mutants designed from the 1D-data-guided model (alt-P4, alt-P5 and alt-P1d in magenta, brown, and red, respectively) give SHAPE profiles in poor agreement with each other, giving no support for these pairings. (B, F) Compensatory mutants designed from the 2D-data-guided model give SHAPE profiles in agreement with the wild type (WT) for shift-P4a (light green) but not shift-P2a (dark green). (C, G) Compensatory mutants give strong support for both P4a (blue) and P2a (cyan). Blue arrows mark G204 exposure in P4a-stabilized mutants. (D) Quartet of electropherograms testing mutation/rescue for P4b (C206G/G213C) does not give support for this pairing. (H–J)  $\chi^2$  score curve of fraction of P4a helix, fitting based on (H) whole RNA (126–235), (I) G204 and A205, and (J) G204 only, using component profiles from P4a-stabilized and shift-P4a-stabilized mutants in (F) and (G). Parameters at which optimal  $\chi^2$  scores are obtained are circled; errors are estimated by values at which  $\chi^2$  increases by one. (K)  $\chi^2$  tests of any additional third state, based on fitting reactivities across whole RNA (126–235) and use of SHAPE profiles for mutants that differed substantially from wild type. All cases show substantial worsening of  $\chi^2$  (by more than one) at >2% population fractions, ruling out significant population fractions of such states.

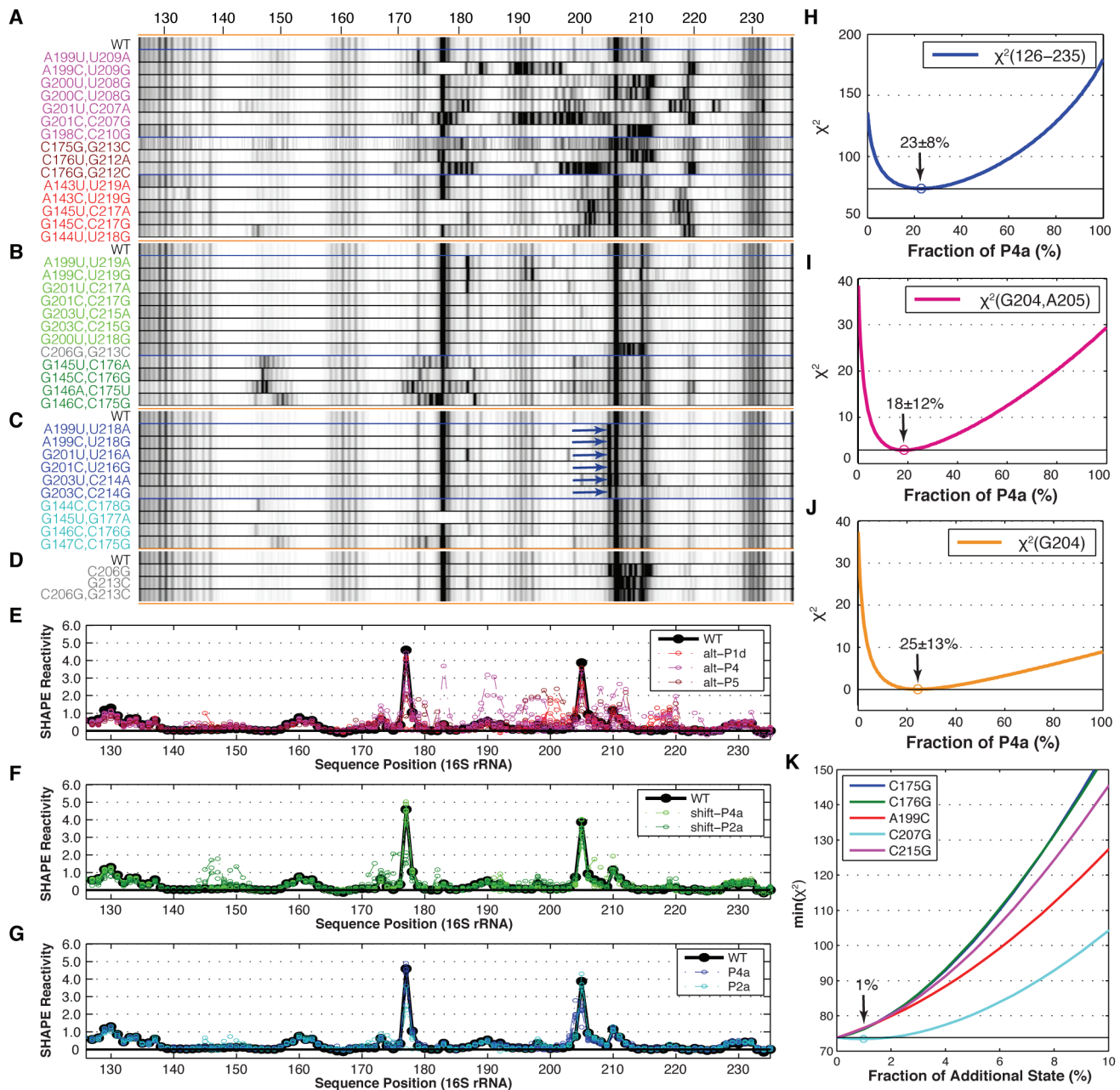


**Figure S5. Repeated SHAPE analysis of M1 and M2 mutants from previous study (Deigan et al. 2009).** (A) Normalized SHAPE reactivity of WT, M1 and M2 resolved by capillary electrophoresis (CE). Flanking sequences are grayed and GAGUA pentaloop highlighted in yellow. Standard deviations (SD) are shown, N = 3. (B) Normalized SHAPE reactivity resolved by next-generation sequencing (MAP-Seq). Error bars are estimated from MAP-Seq raw counts. (C-D) Quartet electropherogram (wild type, single mutants, and double mutant) of M1 (U208C/U218C) and M2 (G145C/U219C). For M1, no significant change is observed, consistent with these mutants preserving the wild type structure. Several models, including a prior model (Deigan et al. 2009) and the distinct secondary structure presented in main text Figure 5 are consistent with these data. For M2, blue arrow marks exposure of G204, consistent with stabilizing crystallographic P4a (the excited state register shift) in this mutant. See main text Discussion for further description.

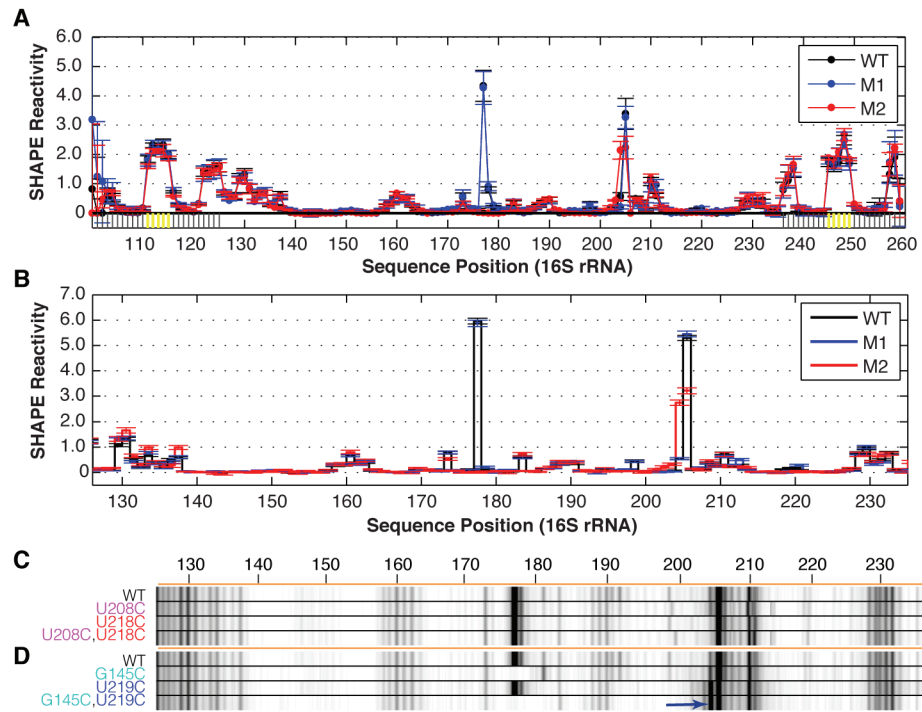
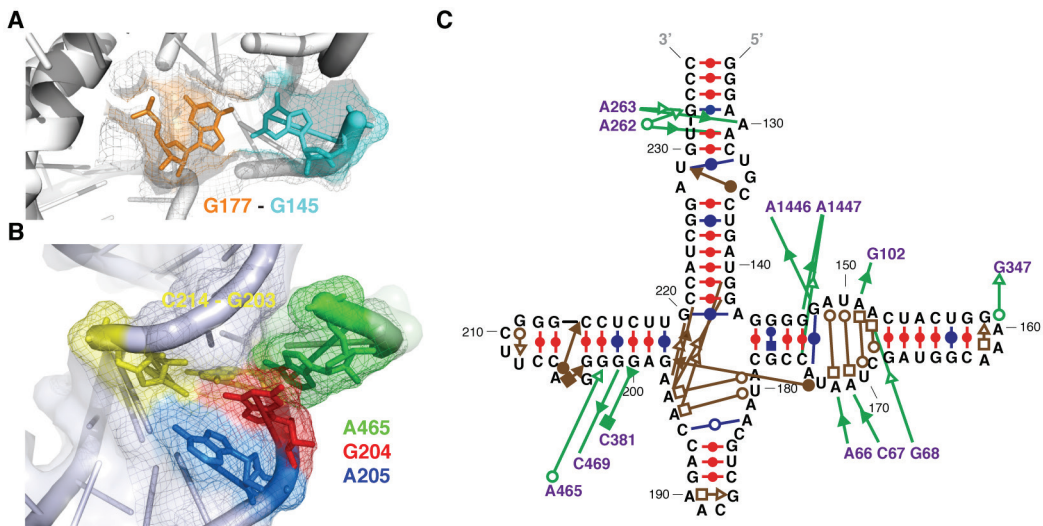


**Figure S6. Non-canonical base-pairs and tertiary contacts intrinsic to the 126-235 RNA or formed during full ribosome assembly.** (A) Base-pairing of G145 and G177 in crystallographic structure may be an intrinsic feature of the 126-235 RNA; the replacement G145C reduces G177 SHAPE reactivity (SI Figure S5D). G177 is in *syn*- conformation and its Hoogsteen edge is forming base-pair with the Watson/Crick edge of G145. (B) RNA-RNA tertiary interaction of P4a that can form in the context of the full 16S rRNA. A-minor contact between A465 and G203/C214 is shown. (C) Secondary structure diagram of 126-235 RNA highlighting contacts with sequences elsewhere in the full-length 16S rRNA using Leontis/Westhof nomenclature (Leontis and Westhof 2001).



## SUPPORTING TABLES

**Table S1. Schematic of PCR primer assembly of wild-type sequence.** A Total of four primers are used to assemble the double stranded DNA template listed in SI Table S2. The annealing sites are shown by vertical lines, annealing temperature for each site is shown on the left. Nucleotide numbering from the full-length 16S rRNA is shown above or under each primer. The forward strand of assembled DNA template is highlighted: T7 promoter (blue), flanking sequences (buffering region / stem of referencing hairpin / pentaloop of referencing hairpin) (yellow/green/red), sequence of interest (black), and tail2 (magenta).

Primers	Sequence
primer-1-F	TTCTAATACGACTCACTATAGGGAACGACTCGAGTAGAGTCGAAAGGGAAACTGCCTGATGGAGGG
primer-2-R	TGCGACGTTATGCGGTATTAGCTACCGTTCCAGTAGTTATCCCCCTCCATCAGGCAGTT
primer-3-F	CCGCATAACGTCGAAGACCAAAGAGGGGACCTCGGGCCTTGCATCGGATGTGCC
primer-4-R	GTTGTTGTTGTTGTTCTTGTGGAGTCTACTCGACTCCTTGGGACATCCGATGGC

**Table S2. List of 16S sequences.** Each sequence composes similar elements (SI Table S1). It starts with a promoter sequence for *in vitro* transcription using T7 RNA polymerase. A 5' flanking sequence contains three Gs to facilitate efficient transcription elongation, a small hairpin (6 base-pairs in the stem and GAGUA pentaloop) for reactivity referencing, as well as four As in buffering region. Followed is the sequence of interest (126-235). A 3' flanking sequence similar to 5' flanking sequence appends, containing three As in buffering region, a small hairpin for reactivity referencing, and AAC buffering the tail2. Tail2 sequence is at the 3' end of each DNA and RNA molecule, which is used to bind the nucleic acid to beads and reverse transcription.

Construct Name	DNA Sequence
16S-WT	TTCTAATACGACTCACTATAGGAACGACTCGAGTAGAGTCGAAAGGGAAACTGCCATGCGATGTGCCAAGGAGTCGAGTAGACTCCAACAAAAGAACACAACAC GCAAGACCAAAGAGGGGGACCTTCGGGCCTTGCATCGGATGTGCCAAGGAGTCGAGTAGACTCCAACAAAAGAACACAACAC
16S-A199T	TTCTAATACGACTCACTATAGGAACGACTCGAGTAGAGTCGAAAGGGAAACTGCCATGCGATGTGCCAAGGAGTCGAGTAGACTCCAACAAAAGAACACAACAC GCAAGACCAAAGTGGGGGACCTTCGGGCCTTGCATCGGATGTGCCAAGGAGTCGAGTAGACTCCAACAAAAGAACACAACAC
16S-T219A	TTCTAATACGACTCACTATAGGAACGACTCGAGTAGAGTCGAAAGGGAAACTGCCATGCGATGTGCCAAGGAGTCGAGTAGACTCCAACAAAAGAACACAACAC GCAAGACCAAAGAGGGGGACCTTCGGGCCTCTAGCCATCGGATGTGCCAAGGAGTCGAGTAGACTCCAACAAAAGAACACAACAC
16S-T218A	TTCTAATACGACTCACTATAGGAACGACTCGAGTAGAGTCGAAAGGGAAACTGCCATGCGATGTGCCAAGGAGTCGAGTAGACTCCAACAAAAGAACACAACAC GCAAGACCAAAGAGGGGGACCTTCGGGCCTCATGCCATCGGATGTGCCAAGGAGTCGAGTAGACTCCAACAAAAGAACACAACAC
16S-A199T;T219A	TTCTAATACGACTCACTATAGGAACGACTCGAGTAGAGTCGAAAGGGAAACTGCCATGCGATGTGCCAAGGAGTCGAGTAGACTCCAACAAAAGAACACAACAC GCAAGACCAAAGTGGGGGACCTTCGGGCCTCTAGCCATCGGATGTGCCAAGGAGTCGAGTAGACTCCAACAAAAGAACACAACAC
16S-A199T;T218A	TTCTAATACGACTCACTATAGGAACGACTCGAGTAGAGTCGAAAGGGAAACTGCCATGCGATGTGCCAAGGAGTCGAGTAGACTCCAACAAAAGAACACAACAC GCAAGACCAAAGTGGGGGACCTTCGGGCCTCATGCCATCGGATGTGCCAAGGAGTCGAGTAGACTCCAACAAAAGAACACAACAC
16S-A199C	TTCTAATACGACTCACTATAGGAACGACTCGAGTAGAGTCGAAAGGGAAACTGCCATGCGATGTGCCAAGGAGTCGAGTAGACTCCAACAAAAGAACACAACAC GCAAGACCAAAGCGGGGGACCTTCGGGCCTTGCATCGGATGTGCCAAGGAGTCGAGTAGACTCCAACAAAAGAACACAACAC
16S-T219G	TTCTAATACGACTCACTATAGGAACGACTCGAGTAGAGTCGAAAGGGAAACTGCCATGCGATGTGCCAAGGAGTCGAGTAGACTCCAACAAAAGAACACAACAC GCAAGACCAAAGAGGGGGACCTTCGGGCCTCTGGCCATCGGATGTGCCAAGGAGTCGAGTAGACTCCAACAAAAGAACACAACAC
16S-T218G	TTCTAATACGACTCACTATAGGAACGACTCGAGTAGAGTCGAAAGGGAAACTGCCATGCGATGTGCCAAGGAGTCGAGTAGACTCCAACAAAAGAACACAACAC GCAAGACCAAAGAGGGGGACCTTCGGGCCTCGCCATCGGATGTGCCAAGGAGTCGAGTAGACTCCAACAAAAGAACACAACAC
16S-A199C;T219G	TTCTAATACGACTCACTATAGGAACGACTCGAGTAGAGTCGAAAGGGAAACTGCCATGCGATGTGCCAAGGAGTCGAGTAGACTCCAACAAAAGAACACAACAC GCAAGACCAAAGCGGGGGACCTTCGGGCCTCTGGCCATCGGATGTGCCAAGGAGTCGAGTAGACTCCAACAAAAGAACACAACAC
16S-A199C;T218G	TTCTAATACGACTCACTATAGGAACGACTCGAGTAGAGTCGAAAGGGAAACTGCCATGCGATGTGCCAAGGAGTCGAGTAGACTCCAACAAAAGAACACAACAC GCAAGACCAAAGCGGGGGACCTTCGGGCCTCGGCCATCGGATGTGCCAAGGAGTCGAGTAGACTCCAACAAAAGAACACAACAC
16S-G201T	TTCTAATACGACTCACTATAGGAACGACTCGAGTAGAGTCGAAAGGGAAACTGCCATGCGATGTGCCAAGGAGTCGAGTAGACTCCAACAAAAGAACACAACAC GCAAGACCAAAGAGTGGGACCTTCGGGCCTTGCATCGGATGTGCCAAGGAGTCGAGTAGACTCCAACAAAAGAACACAACAC
16S-C217A	TTCTAATACGACTCACTATAGGAACGACTCGAGTAGAGTCGAAAGGGAAACTGCCATGCGATGTGCCAAGGAGTCGAGTAGACTCCAACAAAAGAACACAACAC GCAAGACCAAAGAGGGGGACCTTCGGGCCTATTGCCATCGGATGTGCCAAGGAGTCGAGTAGACTCCAACAAAAGAACACAACAC
16S-T216A	TTCTAATACGACTCACTATAGGAACGACTCGAGTAGAGTCGAAAGGGAAACTGCCATGCGATGTGCCAAGGAGTCGAGTAGACTCCAACAAAAGAACACAACAC GCAAGACCAAAGAGGGGGACCTTCGGGCCTTGCCATCGGATGTGCCAAGGAGTCGAGTAGACTCCAACAAAAGAACACAACAC
16S-G201T;C217A	TTCTAATACGACTCACTATAGGAACGACTCGAGTAGAGTCGAAAGGGAAACTGCCATGCGATGTGCCAAGGAGTCGAGTAGACTCCAACAAAAGAACACAACAC GCAAGACCAAAGAGTGGGACCTTCGGGCCTATTGCCATCGGATGTGCCAAGGAGTCGAGTAGACTCCAACAAAAGAACACAACAC
16S-G201T;T216A	TTCTAATACGACTCACTATAGGAACGACTCGAGTAGAGTCGAAAGGGAAACTGCCATGCGATGTGCCAAGGAGTCGAGTAGACTCCAACAAAAGAACACAACAC GCAAGACCAAAGAGTGGGACCTTCGGGCCTTGCCATCGGATGTGCCAAGGAGTCGAGTAGACTCCAACAAAAGAACACAACAC
16S-G201C	TTCTAATACGACTCACTATAGGAACGACTCGAGTAGAGTCGAAAGGGAAACTGCCATGCGATGTGCCAAGGAGTCGAGTAGACTCCAACAAAAGAACACAACAC GCAAGACCAAAGAGCGGGACCTTCGGGCCTTGCCATCGGATGTGCCAAGGAGTCGAGTAGACTCCAACAAAAGAACACAACAC
16S-C217G	TTCTAATACGACTCACTATAGGAACGACTCGAGTAGAGTCGAAAGGGAAACTGCCATGCGATGTGCCAAGGAGTCGAGTAGACTCCAACAAAAGAACACAACAC GCAAGACCAAAGAGGGGGACCTTCGGGCCTTGCATCGGATGTGCCAAGGAGTCGAGTAGACTCCAACAAAAGAACACAACAC
16S-T216G	TTCTAATACGACTCACTATAGGAACGACTCGAGTAGAGTCGAAAGGGAAACTGCCATGCGATGTGCCAAGGAGTCGAGTAGACTCCAACAAAAGAACACAACAC GCAAGACCAAAGAGGGGGACCTTCGGGCCTGGCCATCGGATGTGCCAAGGAGTCGAGTAGACTCCAACAAAAGAACACAACAC
16S-G201C;C217G	TTCTAATACGACTCACTATAGGAACGACTCGAGTAGAGTCGAAAGGGAAACTGCCATGCGATGTGCCAAGGAGTCGAGTAGACTCCAACAAAAGAACACAACAC GCAAGACCAAAGAGCGGGACCTTCGGGCCTGGCCATCGGATGTGCCAAGGAGTCGAGTAGACTCCAACAAAAGAACACAACAC







## SUPPORTING REFERENCES

- Deigan KE, Li TW, Mathews DH, Weeks KM. 2009. Accurate SHAPE-directed RNA structure determination. *Proceedings of the National Academy of Sciences* **106**: 97-102.
- Hajdin CE, Bellaousov S, Huggins W, Leonard CW, Mathews DH, Weeks KM. 2013. Accurate SHAPE-directed RNA secondary structure modeling, including pseudoknots. *Proceedings of the National Academy of Sciences of the United States of America* **110**: 5498-5503.
- Kladwang W, Mann TH, Becka A, Tian S, Kim H, Yoon S, Das R. 2014. Standardization of RNA Chemical Mapping Experiments. *Biochemistry* **53**: 3063-3065.
- Kladwang W, VanLang CC, Cordero P, Das R. 2011. Understanding the errors of SHAPE-directed RNA structure modeling. *Biochemistry* **50**: 8049-8056.
- Leontis NB, Westhof E. 2001. Geometric nomenclature and classification of RNA base pairs. *RNA* **7**: 499-512.